IEEE Access
Multidisciplinary | Rapid Review | Open Access Journal

Received November 24, 2021, accepted December 7, 2021, date of publication December 10, 2021,
date of current version December 20, 2021.

Digital Object Identifier 10.1109/ACCESS.2021.3134497

A Miniaturized Triple-Band and Dual-Polarized Monopole Antenna Based on a CSRR Perturbed Ground Plane

AHMED EL YOUSFI[1], ABDENASSER LAMKADDEM[1], KERLOS ATIA ABDALMALAK[1,2], (Member, IEEE), AND DANIEL SEGOVIA-VARGAS[1], (Member, IEEE)

[1]Signal Theory and Communication Department, University Carlos III of Madrid, 28911 Madrid, Spain
[2]Electrical Engineering Department, Aswan University, Aswan 81542, Egypt

Corresponding author: Ahmed El Yousfi (aelyouf@ing.uc3m.es)

This work was supported by PID2019-109984RB-C41.

ABSTRACT This paper proposes a new triple-band monopole antenna based on Complementary Split Ring Resonators (CSRR) perturbing the ground plane (GND). The antenna consists of an inverted-L-shaped monopole fed by a modified microstrip line with two CSRRs cut out of the ground plane. The operational bands are independently controlled by the CSRR unit cell parameters. In addition, the antenna presents a dual-polarization performance (vertical polarization at 2.4 GHz band and horizontal polarization at both 3.6 and 5.9 GHz bands). The designed antenna is fully planar and low profile avoiding the vias with the ground plane and covering the WLAN, WiMAX, and IEEE 801.11p bands at 2.45, 3.6, and 5.8 GHz. A compact prototype ($0.32\lambda_0 \times 0.32\lambda_0$ being λ_0 is the wavelength corresponding to the lowest resonance frequency) has been fabricated and measured showing good agreement between simulations and measurements. The measured impedance bandwidths are 10% (2.38-2.63 GHz), 2.5% (3.54-3.63 GHz), and 20% (5.83-7.12 GHz) whereas the measured gains are 1.34, 0.68, and 2.65 dBi at 2.4, 3.6, and 5.9 GHz respectively.

INDEX TERMS Complementary split ring resonators (CSRR), monopole antenna, triple-band, dual-polarization, miniaturization.

I. INTRODUCTION

The increasing development of wireless communication systems such as WiMAX and WLAN requires the design of multiband antennas able to operate in different frequency bands. In addition to low profile and wide bandwidth, the antennas should be compact to facilitate their integration with other system components. Printed antennas are a good solution that could fulfill the previous requirements.

Different approaches have been developed in the literature to achieve multi-band property. The most conventional one consists of only acting on the radiating element by inserting conducting strips or etching slots to generate different resonant frequencies [1]-[6]. However, the reported designs either have relatively large dimensions or possess complex structures that can make obtaining the desired frequency a very difficult task. In [6] embedding a set of V slots and slits into an annular patch antenna helps to achieve a triple-band antenna with dual-polarized performance. Despite its compact size ($0.35\lambda \times 0.35\lambda$), the proposed antenna showed relatively narrow bandwidths. In [7], a T-shaped monopole is loaded with a horizontal conducting branch for dual-band radiation. But, the antenna has a large size in addition, the two bands are not independently controlled. In [8], by loading a main radiating patch with four sub patches a multiband performance is achieved with independent frequency control. However, the bands are narrow which is not suitable for applications that need more bandwidth. Parasitic elements have also been used in [9], where T-shaped and Inverted-L strips were placed on a microstrip antenna to achieve multi-band performance but at a cost of a large ground plane and relatively high profile. Another widely used approach [10]–[13]

The associate editor coordinating the review of this manuscript and approving it for publication was Davide Ramaccia.

consists of loading the antenna with Split Ring Resonators (SRR). In [10] and [11], a set of SRR cells were coupled to a slot antenna to obtain multi-band performance but with large dimensions and narrow bandwidth. The same idea was used in [10] but with a dipole with a capacitive gap loaded with via-less composite right/left-handed (CRLH) unit cells to achieve multi-band operation. The CSRR has also been used in [15], [16] for multiband performance in microstrip antennas. However, etching the CSRR in the radiating element decreases both, gain and efficiency. The CSRRs can also be printed in the ground plane for multiband and broadband performances [17]. Additionally, SRRs and CSRRs have been widely used in the filtering antenna design in order to avoid interferences between adjacent bands [18]–[19].

The second approach consists of jointly acting on the ground plane, feeding line, and/or radiating element. In this way, the addition of composite right/left-handed (CRLH) unit cells to load the radiating elements has been proposed to achieve multi-frequency performance with compact size [20]–[22]. However, this structure needs bridges in the coplanar feeding line and vias to the ground plane what makes the manufacturing process much more complicated. In [23], a triple-band monopole antenna was achieved by loading the monopole with distributed CRLH lines. However, the resultant radiation pattern is not monopolar within all operating bands. Finally, in [24], a bulky 3-D miniaturized monopole antenna was achieved. It consists of a vertical monopole loaded with a CSRR plus multiple zeroth-order resonator (ZOR) unit cells over the ground plane to achieve multi-band performance with an independent tuning of the frequencies band. However, the profile of the antenna is relatively high (0.1λ) and the bandwidth is narrow.

In this paper, a fully planar multi-band monopole antenna is presented thanks to jointly working on the whole antenna: radiating element and ground plane. In this way, the inclusion of a pair of CSRRs in the microstrip feeding line will constitute a defected ground plane and provide additional horizontally polarized resonances. In comparison with previously stated works this antenna has a low profile and shows large compactness and is easier to manufacture due to its fully planar structure. The inclusion of the CSRRs in the ground plane perturbs the current distribution in a coherent way creating an in-phase current along the x-axis at 3.6 and 5.9 GHz what contributes to the radiation. Consequently, a triple-band independently controlled resonance can be achieved by modifying the dimensions of the CSRRs in the defected ground plane. Finally, the proposed antenna provides a dual-polarized performance: vertical polarization at 2.4 GHz associated with the vertical radiating element and dual-band horizontal polarization at 3.6 and 5.9 GHz associated with the perturbed GND.

The rest of the paper is organized as follows: Section II presents the operation principle of the antenna and its design process, current distribution, parametric study, and equivalent circuit. The experimental results that validate the simulations are shown in Section III. Section IV contains a conclusion.

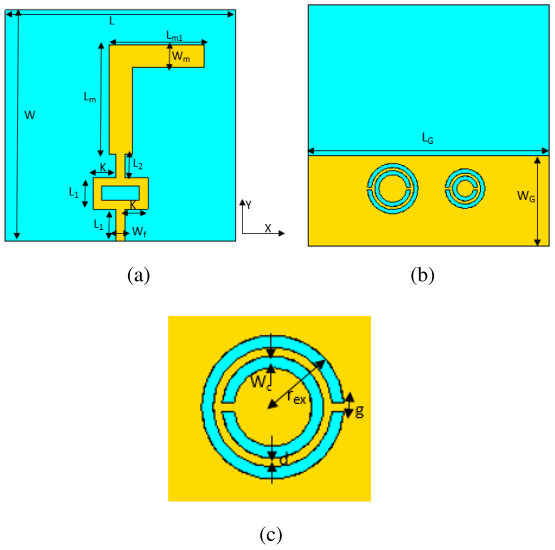

FIGURE 1. Proposed tiple band antenna (a) top view (b) back view (c) CSRR unit cell.

II. ANTENNA DESIGN

A. ANTENNA DESIGN

The proposed triple-band antenna geometry is shown in Fig. 1. The antenna consists of two layers. The top layer contains an inverted L-shape monopole designed to resonate at 2.4 GHz. A forked-like microstrip feeding line has been added to also consider the ground plane. Secondly, in the bottom layer, two CSRRs cells with different sizes have been etched out from a partial ground plane to achieve multi-band performance. The two rings in the CSRRs keep the same slot's width and the gap at the end of the slot. The only different dimensions are the external radius r_{ex} and r_{ex1} which belongs to the small and large CSRR respectively as shown in Fig. 1. It is important to emphasize that if it were not for the forked feeding line the two CSRRs would not be equally excited neither in amplitude nor in phase. This feeding strategy allows the triple-band performance. We note that such a microstrip feeding line is selected to solve the problem of the beam tilt and gain decrease. This has been shown in [17] where a meandered microstrip feeding line was used for exciting two CSRR to obtain dual broadband performance. Therefore, out-of-phase currents are excited at a higher frequency band, which led to a great decrease of the broadside gain. This feeding approach can be extended to other metamaterial unit cells such as rectangular CSRR where the same radiation performances are obtained.

A further explanation of the way that the antenna works can be given by splitting the design steps of the proposed antenna. This is illustrated in Fig. 2 where all the design steps are presented. Firstly, the single inverted L-shaped monopole antenna denoted as Ant 0 refers to the conventional basic antenna without CSRR loading. This inverted L-shaped monopole provides the lowest working frequency, in this case, 2.4 GHz, and is fed through a straight microstrip line. This resonance is calculated when the length of the

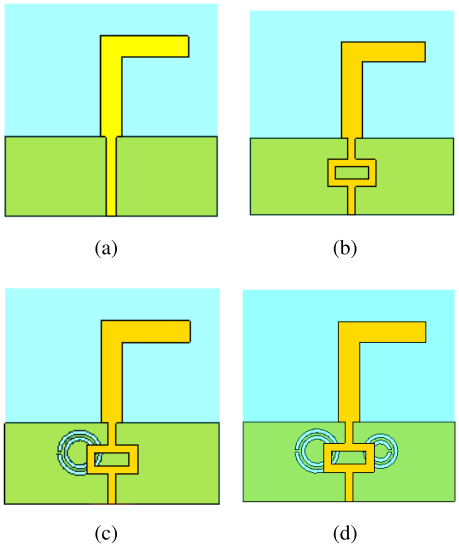

FIGURE 2. Design steps of the proposed antenna (a) Ant 0 (b) Ant 1 (c) Ant 2 (d) Prop Ant.

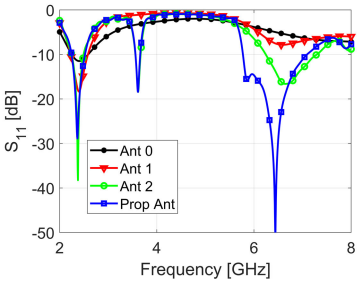

FIGURE 3. Simulated return loss for different antennas.

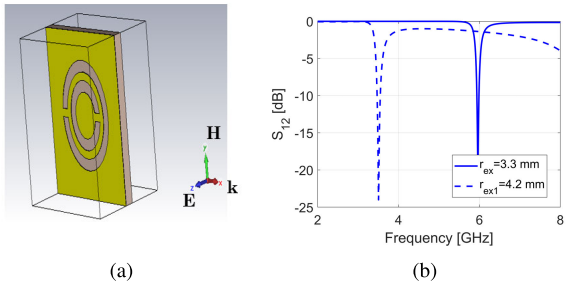

FIGURE 4. Simulation set up (a) CSRR unit cell (b) S_{12} of the two CSRRs.

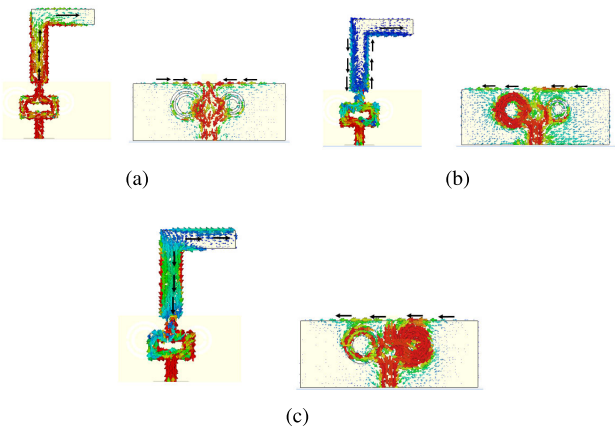

FIGURE 5. The current distribution of the proposed antenna: on the monopole (left) and ground plane (right) at (a) 2.4 GHz (b) 3.6 GHz (c) 5.9 GHz.

monopole (L_m+L_{m1}) is approximately $\lambda_g/4$ (λ_g guided wavelength at 2.4 GHz) which corresponds to the fundamental mode of a conventional monopole antenna. Secondly, the inclusion of the forked-like feeding line constitutes the so-called Ant 1. This structure is designed to allow the presence of a tiny resonance at the highest desired frequency, in this case in the 6 GHz band. Thirdly, the perturbed ground plane (GND) is achieved through etching out one CSRR in the GND. This structure is called Ant 2 and the CSRR is designed to provide resonance at the intermediate WIMAX band, in this case, 3.6 GHz as shown in Fig. 3. Finally, in order to symmetrize the antenna and improve the performance at the highest frequency, another CSRR has been etched out at the other prong of the forked-like feeding line. This will constitute the so-called Prop Ant and is shown in Fig. 2. Moreover, it can be seen that not only does the inclusion of the CSRR in the GND preserve the performance of the base monopole but also improves the matching conditions and enlarges its impedance bandwidth.

The fundamental mode of the CSRR unit cell is excited when an axial electric field is applied [25]. Thus, two CSRR unit cells with two different radii have been simulated as shown in Fig. 4. From Fig. 4 (b), it can be seen that the two resonances agree well with the obtained results in Fig. 3 where the two CSRRs are inserted below the feeding line.

Concerning the radiation mechanism, it can be seen that the high frequencies (3.6 and 5.9 GHz) are not any longer due to the monopole effect but to the perturbed ground plane. Then, despite of providing vertical polarization the final triple frequency antenna will provide two horizontal polarizations associated with the perturbed GND and one vertical polarization associated with the folded monopole. The resulting antenna covers the standard IEEE 802.11p. It can also be noted that the fundamental and higher modes of the monopole have been slightly shifted down due to the capacitive effect between the monopole itself and the loaded CSRR.

To gain more insight into the radiation mechanism of the proposed antenna, the current distribution at each resonant frequency is being analyzed through a full-wave simulation with CST. The designed frequencies are 2.4 G, 3.6, and 5.9 GHz respectively. Fig. 5 (a)-(c) shows the current distribution at the previous frequencies. At 2.4 GHz, we can see that the current distribution on the inverted L shape is similar to that of the reference monopole antenna (Ant 0). For the sake of conciseness, the current distribution at 2.4 GHz of the reference antenna (Ant 0) is not presented. The presence of the CSRR in the perturbed GND causes to appear two out of phase currents along with the GND. These currents are then canceled out and do not contribute to the overall radiation

TABLE 1. Optimized dimensions of the proposed antenna.

Param	L_m	L_{m1}	L_g	W_g	W	L	W_m	r_{ex1}
Value (mm)	19	13	40	15	40	40	4	4.2
Param	W_f	K	W_c	d	g	L_1	L_2	r_{ex}
Value (mm)	1.5	4	0.7	0.5	0.5	5.5	4	3.3

resulting in a vertically polarized E field. At 3.6 GHz, the radiation mechanism is somewhat different since the currents on the vertical monopole are very small and are canceled out due to its out-of-phase distribution. Then, the large currents surrounding the left CSRR (the CSRR with large dimension) induce a net in-phase current distribution along the edge of the ground plane along the x-axis. This yields to somewhat dipole-like radiation oriented along the x-axis. This fact will be demonstrated in the next section by giving the radiation pattern. Finally, at the highest frequency band, the current distribution on the vertical monopole produces a notch just at the middle of the monopole what yields to a tiny higher-order vertical mode as can be appreciated around 7.8 GHz. In addition to that, the presence of the large current distribution surrounding the small CSRRs (the one on the right) induces a horizontal current along the x-axis resulting in a dipole-like radiation pattern. It is also seen that these currents along the horizontal edge of the ground plane contribute to the radiation since they are in phase as can be seen in Fig. 5 (c). One of the advantages of this proposed antenna is that it exhibits an independent control of the resonance frequencies. In order to demonstrate this characteristic, a parametric study of some key parameters will be shown in the next subsection.

B. SIMULATED ANTENNA: PARAMETRIC STUDY AND EQUIVALENT CIRCUIT

The proposed antenna has been designed and printed on a thin Rogers with a dielectric constant of 2.2, loss tangent 0.0009, and thickness h=0.787 mm. The design parameters can be found in Fig. 1 and have been chosen to achieve a multifrequency antenna working at 2.4, 3.6, and 5.9 GHz. Table 1 provides the dimensions of all the design parameters.

Once the design has been done, a parametric study of the most critical parameters has been undertaken. As the triple frequency performance is greatly associated with the CSRR, the outer radii of the CSRRs will be studied. Fig. 6 (a) illustrates the effect of the outer radius of the large CSRR on the return losses of the proposed antenna. As r_{ex1} increases, the second resonance at 3.6 GHz shifts down toward lower frequencies while other resonances remain almost unchanged. We can see another resonance at around 7.5 GHz which behaves like the previous one. This resonance is associated to the higher mode of the CSRR. A fine optimization of this resonance may lead to broadening more the highest frequency band.

Fig. 6 (b) shows that the outer radius of the small CSRR, r_{ex}, mostly affects the upper band. It is seen that the first

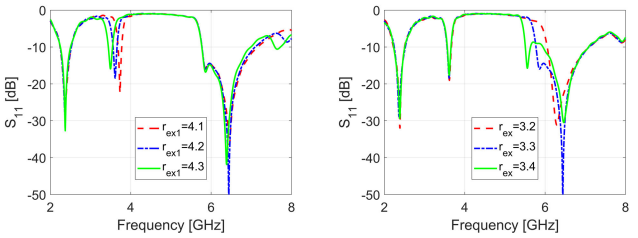

FIGURE 6. The simulated return loss of the proposed antenna for different (a) r_{ex1} (b) r_{ex} values.

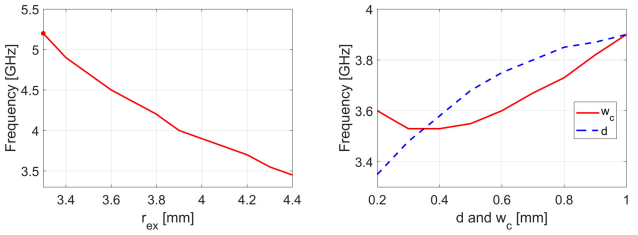

FIGURE 7. Effect of CSRR dimensions on the second resonance frequency (a) r_{ex} (b) w_c and d.

resonance shifts down to lower frequencies with increasing r_{ex}, while the second resonance shifts up to higher frequencies. This provides the ability to achieve different working bands just by controlling the outer radius of the CSRRs. These results reveal that the two resonances could be separately tuned without affecting the first one that can be easily controlled by the inverted L monopole.

It is worth noting that other applications such as WLAN 2.4/5.2/5.8 GHz can be easily obtained by changing the CSRR parameters: outer radius r_{ex}, strip width d, and slot width w_c as shown in Fig. 7. We note that when one parameter is changed the others are kept at their optimized values. It is seen that when r_{ex} increases from 3.3 to 4.4 mm the frequency is shifted from 5.2 to 3.45 GHz (Fig. 7 (a)). This is due to the decrease of the equivalent capacitance of CSRR C_{csrr} since it can be modeled as an LC resonator tank as shown in Fig. 8. On the other hand, w_c and d have similar behavior over the frequency band but in an opposite way (Fig. 7(b)). Increasing d decreases the equivalent inductance of CSRR L_{csrr} while increasing w_c decreases the capacitance C_{csrr} leading to a shift of frequency to higher values. This is consistent with the theoretical analysis reported in [25].

In order to have a more accurate control on all the resonance frequencies of the triple-band antenna, an equivalent circuit based on lumped elements has been proposed. The equivalent circuit is composed of four resonant circuits and their corresponding couplings between them. According to [25] two CSRRs have been modeled as shown in Fig. 8. Therefore a CSRR unit cell can be modeled as two L and C parallel circuit. First, a capacitor and an inductor, C_f and L_f, are needed to model the microstrip feeding line. Secondly,

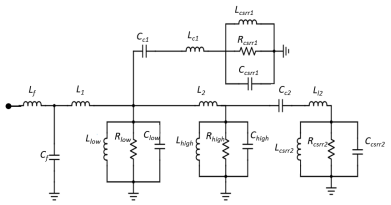

FIGURE 8. Equivalent circuit model of the proposed loaded monopole.

TABLE 2. Optimized values of the proposed circuit.

L_f (nH)	L_1 (nH)	C_f (pF)	L_{low} (nH)	C_{low} (pF)	R_{low} (Ω)	C_{c1} (pF)
0.3	0.69	1.017	6.4	2.32	50	0.41
R_{csrr1} (kΩ)	L_2 (nH)	L_{high} (nH)	R_{high} (Ω)	C_{high} (pF)	C_{c2} (pF)	L_{l2} (nH)
1.26	0.82	0.7	37.5	1.14	0.23	3.03
C_{csrr1} (pF)	R_{csrr2} (kΩ)	L_{c1} (nH)	L_{l1} (nH)	L_{csrr1} (nH)	L_{csrr2} (nH)	C_{csrr2} (pF)
0.45	3.3	0.137	0.13	0.9	1.78	0.7

four resonant parallel circuits are placed to model the CSRRs in the ground plane and the two resonant frequencies of the monopole. Then, the resonance frequency of the CSRR at 3.6 GHz is modeled with C_{csrr2}, R_{csrr2}, L_{csrr2} elements for the lowest resonant frequency, and C_{csrr1}, R_{csrr1}, L_{csrr1} for the highest resonance frequency of the CSRR at 5.8 GHz. In addition to that, two other resonators associated to the monopole have been also modeled as C_{low}, L_{low}, R_{low} and C_{high}, L_{high}, R_{high} respectively. Finally, the coupling between CSRR cells with the feeding line is realized through C_{c1}, L_{l1}, C_{c2}, and L_{l2}. Another two inductors, L_1 and L_2, have been added to take into account the joint between the feeding lines and the monopole for the lowest and highest frequencies respectively. It is important to note that the resonance frequencies associated with the two CSRRs are mainly affected by the capacitive coupling between the fork-like feeding line and CSRRs. Therefore, the resonance frequency is given by:

$$f_r = 1/2\pi\sqrt{L_{cssrr}(C_{csrr} + C_c)} \quad (1)$$

This results in the following resonances of 5.6 and 3.9 GHz for CSRR1 and CSRR2 respectively, which are slightly shifted from the simulated results shown in Fig. 10 due to the effect of the rest of the circuit. The optimized parameters of the circuit model are given in table 2.

The results of the equivalent circuit, CST MW solver, and measurements are depicted in Fig. 10. A good agreement can be seen between all of them.

III. SIMULATED AND MEASURED RESULTS

To experimentally validate the performances of the proposed antenna, a prototype has been fabricated based on the optimized values given in Table 1. The manufactured prototype can be seen in Fig. 9. Fig. 10 shows the simulated and measured results of the return loss versus frequency of the proposed tri-band antenna. A good agreement is observed, the small discrepancy can be attributed to fabrication errors and

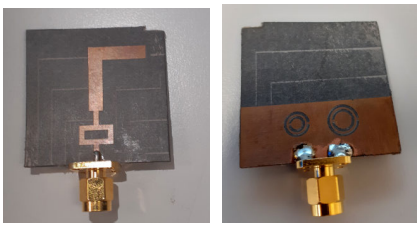

(a) (b)

FIGURE 9. Fabricated prototype of the proposed antenna (a) top view (b) back view.

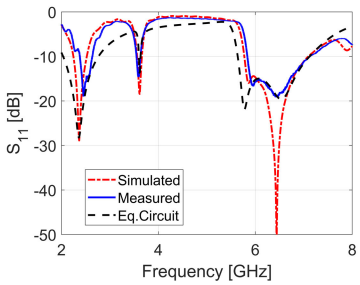

FIGURE 10. Simulated and measured return loss of the proposed antenna.

measurement conditions. The measured -10 dB bandwidth is about 250 MHz (2.38-2.63 GHz) for the first resonance which covers 2.4/2.5 GHz WLAN and WiMAX operation bands, 90 MHz (3.54-3.63 GHz) for the middle resonance which covers a part of the 3.5 GHz WiMAX band and 1.29 GHz (5.83-7.12 GHz) for the upper resonant frequency covering the requirement of IEEE 802.11p standard (5.850-5.925 GHz). The measurement setup of the radiation pattern is shown in Fig. 11 (a). The simulated and measured radiation patterns of the proposed antenna at each resonant frequency are given in Fig. 12. A good agreement has also been achieved except for some discrepancies that may be attributed to the measurement conditions. We note that the presence of the unavoidable metallic holder behind the antenna causes to appear some ripples in the radiation pattern. Thus, an absorbing material has been added between the antenna and the holder to isolate them and avoid such ripples. It is important to note that due to the presence of the absorber the measurements have only been taken in the range $\pm 90°$ since the back radiations are absorbed and suppressed.

Figure 12 (a) and (b) present the radiation pattern of the proposed antenna at 2.4 GHz. As it was previously expected in Fig. 5 (a) the antenna exhibits omnidirectional and bidirectional radiations in XZ and YZ planes respectively which are consistent with the radiation of a conventional monopole antenna in which the y-directed currents are the main contributors to the radiation. The cross-polarization level at the broadside direction is lower than -15 dB. At 3.6 GHz the antenna provides an orthogonal polarization to the one obtained at 2.4 GHz as shown in Fig. 12 (c) and (d). In this case, the antenna exhibits omnidirectional and bidirectional

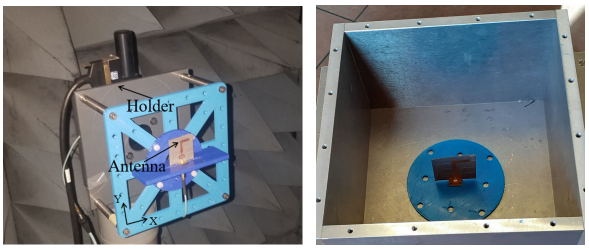

(a) (b)

FIGURE 11. Measurement setup of (a) radiation pattern (b) radiation efficiency.

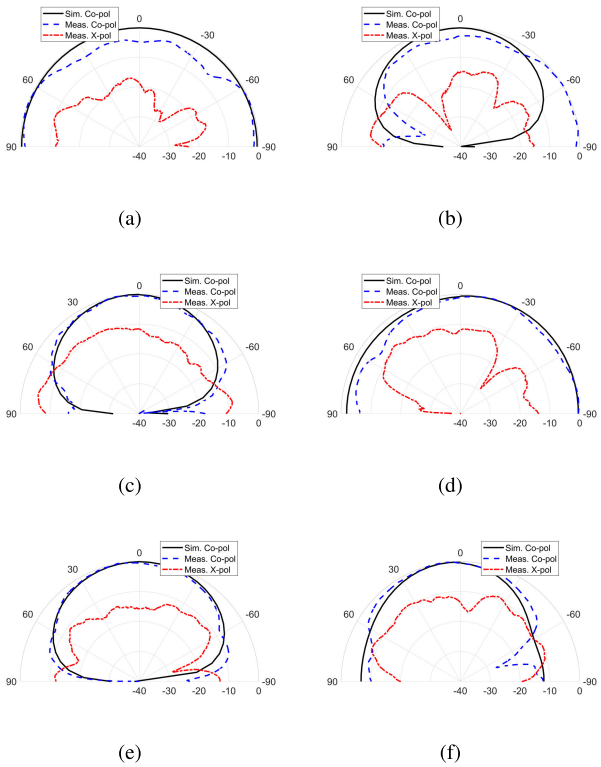

(a) (b) (c) (d) (e) (f)

FIGURE 12. Simulated and measured radiation pattern in the planes (a) XZ and (b) YZ at 3.6 GHz (c) XZ (d) YZ at 3.6 GHz (e) XZ (f) YZ at 5.9 GHz.

radiations in YZ and XZ planes respectively which means that the radiation is due to the in-phase x-directed currents in the ground plane as shown in Fig. 5 (b). The currents along the y-axis in the monopole contribute to the cross-polarization. The cross-polarization level is lower than −12 dB at the broadside direction. At 5.9 GHz, the radiation pattern is similar to the one obtained at 3.6 GHz as can be observed in Fig. 12 (e) and (f), with a cross-polarization difference larger than −15 dB at the broadside direction.

The radiation efficiency was measured using the Wheeler cap method [28]. The Wheeler cap is a rectangular cavity with dimensions 20×20×14 cm^3. With this size, the corresponding resonance frequency of the cap is 1.06 GHz which is below the operating frequency bands of our antenna. The position of the antenna inside the Wheeler cap is in the

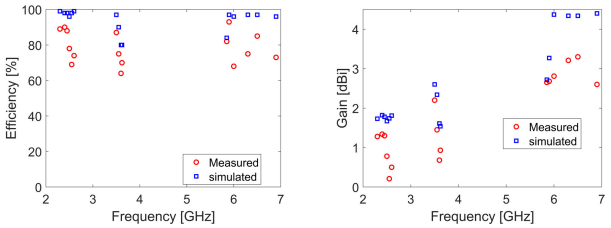

(a) (b)

FIGURE 13. Measured and simulated (a) radiation efficiency (b) broadside gain.

TABLE 3. Comparison with recent works.

Ref	Freq (GHz)	-10dB band (%)	Gain (dBi)	Polari-zation	Height (λ_0)	Size ($\lambda_0{}^2$)	Technique
[26]	3.04 3.83 4.83 5.76	0.82 0.65 0.81 0.71	2.36 1.43 2.11 2.39	Single LP	0.019	0.4 × 0.4	Shorting pins with multiple U slots
[27]	4.56 5.02 5.48	1.53 0.4 0.36	5.65 5.9 5.02	Single LP	0.024	0.75 × 0.51	HMSIW
[20]	5.17	78.5	NA	Dual LP	0.018	0.26 × 0.35	NRI TL with via
[21]	2.45 3.5 5.5	3.67 17.7 32	0.98 1.25 2.05	Dual LP	0.012	0.32 × 0.2	TL MTM With vias and bridges
[24]^a	2.1 3.1 4.8	0.66 0.67 1.08	-3.6 1.3 4.7	Single LP	0.1	NA	ZOR and CSRR loading with vias
[24]^b	2.1 3.1 4.8	5.6 0.3 0.7	1.2 0.7 5.6	Single LP	0.1	NA	ZOR and CSRR loading with vias
[7]	2.37 5.18	16.5 2	1.3 0.8	Single LP	0.006	0.59 × 0.59	T monopole loaded with horizontal strip
[29]	4.27 4.85 6.45	2.8 3.3 3.9	1.76 2.3 1.45	Single LP	0.027	0.45 × 0.57	Monopole loaded with meandred strips
Our work	**2.4 3.6 6.47**	**10 2.50 20**	**1.34 0.68 2.65**	**Dual LP**	**0.006**	0.32 × 0.32	**CSRR loading without vias**

middle and is presented in Fig. 11 (b). The method consists of two main measures. The first one measures the S_{11} of the proposed antenna in a free space environment. The second one measures the antenna when enclosed in the Wheeler cap so that any radiation can be eliminated. The measured and simulated radiation efficiency over the frequency is shown in Fig. 13 (a). The measurements show an efficiency of 90%, 64%, and 93% at 2.4, 3.6, and 5.9GHz respectively which well agree with the simulated ones (98%, 75%, and 97%).

The estimated measured gain based on the measured efficiency and the simulated directivity is calculated using equation 2

$$G_{estimated} = D_{simulated} * \eta_{measured} \tag{2}$$

Based on that, the estimated measured gain and simulated gain as a function of frequency are shown in Fig. 13 (b).

It is clearly seen that the estimated measured gain is 1.34, 0.68, and 2.65 dBi at 2.4, 3.6, and 5.9 GHz respectively which agree well with the simulated results 1.78, 1.28, and 4.13 dBi at the same operating frequencies.

A comparison between the proposed antenna and some recent works is given in Table 3. The designs in [26] and [27] present high gain at the operating frequencies but at the cost of large size and narrow bandwidths which may limit their application. References [7] and [29] are single structures only based on strip loading but with large size and single polarization. Finally, references [20] and [21] have dual LP with a small horizontal size but with vias and bridges that make its profile higher and more complex than the one presented here.

From this comparison, it is concluded that the proposed antenna presents the lowest and most simple profile with dual linear polarization characteristic (LP) and good bandwidth.

IV. CONCLUSION

A novel tri-band antenna based on CSRR loading is studied. By etching out two CSRRs in the ground plane of an inverted L-shaped monopole and modifying the geometry of the feeding line the antenna can cover three working bands for WLAN, WiMAX, and IEEE 802.11p applications. Additionally, the CSRRs allow independent control of the obtained frequency bands. The simulated results have been verified through measurements of a fabricated antenna prototype. The proposed antenna exhibits good radiation performance in terms of gain, efficiency, and radiation patterns. Furthermore, having a low profile, compact size, and simple structure for ease of implementation with other devices. The proposed antenna could be suitable for modern wireless communication systems.

REFERENCES

[1] L. C. Tsai, "Design of triple-band T-U-shaped CPW-FED slot antennas," *Microw. Opt. Technol. Lett.*, vol. 56, no. 4, pp. 844–848, Apr. 2014.

[2] J. Park, M. Jeong, N. Hussain, S. Rhee, P. Kim, and N. Kim, "Design and fabrication of triple-band folded dipole antenna for GPS/DCS/WLAN/WiMAX applications," *Microw. Opt. Technol. Lett.*, vol. 61, no. 5, pp. 1328–1332, 2019.

[3] P. Wang, G. J. Wen, Y. J. Huang, and Y. H. Sun, "Compact CPW fed planar monopole antenna with distinct triple bands for WiFi/WiMAX applications," *Electron. Lett.*, vol. 48, no. 7, pp. 357–359, Nov. 2012.

[4] Y.-D. Wang, J.-H. Lu, and H.-M. Hsiao, "Novel design of semi-circular slot antenna with triple-band operation for WLAN/WIMAX communication," *Microw. Opt. Technol. Lett.*, vol. 50, no. 6, pp. 1531–1534, Jun. 2008.

[5] R. Sonak, M. Ameen, and R. K. Chaudhary, "CPW-fed electrically small open-ended zeroth order resonating metamaterial antenna with dual-band features for GPS/WiMAX/WLAN applications," *AEU Int. J. Electron. Commun.*, vol. 104, pp. 99–107, May 2019.

[6] S. Mathew, M. Ameen, M. P. Jayakrishnan, P. Mohanan, and K. Vasudevan, "Compact dual polarised V slit, stub and slot embedded circular patch antenna for UMTS/WiMAX/WLAN applications," *Electron. Lett.*, vol. 52, no. 17, pp. 1425–1426, Aug. 2016.

[7] Y.-L. Kuo and K.-L. Wong, "Printed double-T monopole antenna for 2.4/5.2 GHz dual-band WLAN operations," *IEEE Trans. Antennas Propag.*, vol. 51, no. 9, pp. 2187–2192, Sep. 2003.

[8] H. F. Abutarboush, R. Nilavalan, S. W. Cheung, and K. M. Nasr, "Compact printed multiband antenna with independent setting suitable for fixed and reconfigurable wireless communication systems," *IEEE Trans. Antennas Propag.*, vol. 60, no. 8, pp. 3867–3874, Aug. 2012.

[9] J.-W. Kim, T.-H. Jung, H.-K. Ryu, J.-M. Woo, C.-S. Eun, and D.-K. Lee, "Compact multiband microstrip antenna using inverted-L- and T-shaped parasitic elements," *IEEE Antennas Wireless Propag. Lett.*, vol. 12, pp. 1299–1302, 2013.

[10] P. M. Paul, K. Kandasamy, and M. S. Sharawi, "A tri-band slot antenna loaded with split ring resonators," *Microw. Opt. Technol. Lett.*, vol. 59, no. 10, pp. 2638–2643, 2017.

[11] P. M. Paul, K. Kandasamy, and M. S. Sharawi, "A triband circularly polarized strip and SRR-loaded slot antenna," *IEEE Trans. Antennas Propag.*, vol. 66, no. 10, pp. 5569–5573, Oct. 2018.

[12] F. J. Herraiz-Martínez, L. E. García-Muñoz, D. González-Ovejero, V. González-Posadas, and D. Segovia-Vargas, "Dual-frequency printed dipole loaded with split ring resonators," *IEEE Antennas Wireless Propag. Lett.*, vol. 8, pp. 852–855, 2014.

[13] R. Sonak, M. Ameen, and R. K. Chaudhary, "Triple band omnidirectional miniaturized metamaterial inspired antenna using flipped rectangular stub for LTE, WiMAX, and WLAN applications," *Int. J. RF Microw. Comput.-Aided Eng.*, vol. 29, no. 7, Jul. 2019, Art. no. e21721.

[14] K. Saurav, D. Sarkar, and K. V. Srivastava, "CRLH unit cell loaded multiband printed dipole antenna," *IEEE Antennas Wireless Propag. Lett.*, vol. 13, pp. 852–855, 2009.

[15] N. Ortiz, F. Falcone, and M. Sorolla, "Dual Band patch antenna based on Complementary split ring resonator," in *Proc. Asia Pacific Microw. Conf. (APMC)*, Singapore, Dec. 2009, pp. 2762–2765.

[16] S. C. Basaran, U. Olgun, and K. Sertel, "Multiband monopole antenna with complementary split-ring resonators for WLAN and WiMAX applications," *Electron. Lett.*, vol. 49, no. 10, pp. 1516–1517, May 2013.

[17] A. E. Yousfi, A. Es-salhi, A. Lamkaddem, D. Segovia-Vargas, M. A. Ennasar, and O. E. Mrabet, "A miniaturized multiband monopole antenna with CSRR loaded on ground plane," in *Proc. IEEE Int. Symp. Antennas Propag. North Amer. Radio Sci. Meeting*, Jul. 2020, pp. 1961–1962.

[18] M. S. A. Rani, S. K. A. Rahim, M. R. Kamarudin, T. Peter, S. W. Cheung, and B. M. Saad, "Electromagnetic behaviors of thin film CPW-fed CSRR loaded on UWB transparent antenna," *IEEE Antennas Wireless Propag. Lett.*, vol. 13, pp. 1239–1242, 2014.

[19] M. Barbuto, F. Trotta, F. Bilotti, and A. Toscano, "Horn antennas with integrated notch filters," *IEEE Trans. Antennas Propag.*, vol. 63, no. 2, pp. 781–785, Feb. 2015.

[20] M. A. Antoniades and G. V. Eleftheriades, "A broadband dual-mode monopole antenna using NRI-TL metamaterial loading," *IEEE Antennas Wireless Propag. Lett.*, vol. 8, pp. 258–261, 2009.

[21] J. Zhu, M. A. Antoniades, and G. V. Eleftheriades, "A compact tri-band monopole antenna with single-cell metamaterial loading," *IEEE Trans. Antennas Propag.*, vol. 58, no. 4, pp. 1031–1038, Apr. 2010.

[22] A. A. Ibrahim and A. M. E. Safwat, "Microstrip-fed monopole antennas loaded with CRLH unit cells," *IEEE Trans. Antennas Propag.*, vol. 60, no. 9, pp. 4027–4036, Sep. 2012.

[23] S. Jamilan, M. A. Antoniades, J. Nourinia, and M. N. Azarmanesh, "A directivity band dependent triple band and wideband dual-polarized monopole antenna loaded with a via free CRLH unit cell," *IEEE Antennas Wireless Propag. Lett.*, vol. 14, pp. 855–858, 2015.

[24] A. Mehdipour, T. A. Denidni, and A.-R. Sebak, "Multi-band miniaturized antenna loaded by ZOR and CSRR metamaterial structures with monopolar radiation pattern," *IEEE Trans. Antennas Propag.*, vol. 62, no. 2, pp. 555–562, Feb. 2014.

[25] J. D. Baena, J. Bonache, F. Martin, R. M. Sillero, F. Falcone, T. Lopetegi, M. A. G. Laso, J. Garcia-Garcia, I. Gil, M. F. Portillo, and M. Sorolla, "Equivalent-circuit models for split-ring resonators and complementary split-ring resonators coupled to planar transmission lines," *IEEE Trans. Microw. Theory Tech.*, vol. 53, no. 4, pp. 1451–1461, Apr. 2005.

[26] A. Boukarkar, X. Q. Lin, Y. Jiang, and Y. Q. Yu, "Miniaturized single-feed multiband patch antennas," *IEEE Trans. Antennas Propag.*, vol. 65, no. 2, pp. 850–854, Feb. 2017.

[27] X. Yang, L. Ge, Y. Ji, X. Zeng, and K. M. Luk, "Design of low-profile multi-band half-mode substrate-integrated waveguide antennas," *IEEE Trans. Antennas Propag.*, vol. 67, no. 10, pp. 6639–6644, Oct. 2019.

[28] W. E. McKinzie, "A modified wheeler cap method for measuring antenna efficiency," in *IEEE Antennas Propag. Soc. Int. Symp. Dig.*, Jul. 1997, pp. 542–545.

[29] A. Iqbal, A. Bouazizi, O. A. Saraereh, A. Basir, and R. K. Gangwar, "Design of multiple band, meandered strips connected patch antenna," *Prog. Electromagn. Res. Lett.*, vol. 79, pp. 51–57, 2018.

AHMED EL YOUSFI was born in Al Hoceima, Morocco. He received the double bachelor's degree in physics from the University of Lille 1 Sciences and Technology, France, and Mohamed I University, Oujda, Morocco, in 2016, and the master's degree in electronics and telecommunications engineering from the Abdelmalek Essaâdi University of Tétouan, Morocco, in 2017. He is currently pursuing the Ph.D. degree with the Group of Radiofrequency, Electromagnetics, Microwaves, and Antennas (GREMA), Carlos III University of Madrid (UC3M). In 2020, he joined the Signal Theory and Communication Department, UC3M, as a Teaching Assistant. He worked on massive MIMO antenna for Huawei Project. He has authored/coauthored several international conference papers. His research interests include multiband/broadband antennas based on metamaterials, characteristic mode analysis for metasurface antennas, array antennas for 5G applications, and implantable antennas. He received an Erasmus+ Grant, in 2019. He served as a Peer Reviewer for *European Conference on Antennas and Propagation* (EuCAP).

ABDENASSER LAMKADDEM was born in El Aioun Sidi Mellouk, Morocco, in 1993. He received the B.S. degree from Mohamed I University, Oujda, Morocco, in 2014, and the M.S. degree in communication systems and embedded electronics from Abdelmalek Essaadi University, Tanger, Morocco, in 2016. He is currently pursuing the Ph.D. degree with Carlos III University, Madrid, Spain. He was a Visiting Student with the Department of Signal Theory and Communications, Madrid. He has participated in several research projects financed by Telnet and Huawei. He has authored/coauthored several international conference papers. His current research interests include implantable antennas and wireless power transfer for biomedical applications, small antennas, antenna array for 5G applications, ultra-wideband antennas, reconfigurable antennas, EBG, and frequency selective surfaces. He received the Erasmus+ Grant, in 2019.

KERLOS ATIA ABDALMALAK (Member, IEEE) received the B.Sc. degree (Hons) in communication engineering from Aswan University, Egypt, in 2011, ranked second among the colleagues, and the M.Sc. degree (Hons.) in multimedia and communication from the Carlos III University of Madrid, in 2015, where he is currently pursuing the Ph.D. degree with the Department of Signal Theory and Communications.

In 2011, he joined the Department of Electrical Engineering, Aswan University, as a Teaching Assistant. He has authored/coauthored 11 Journal Citation Ranking "JCR" journals (seven in the first quartile Q1 and three in the second quartile Q2 following Thomson Reuters), two invited papers, and 30 international conference papers. He has participated in 12 research projects financed by Madrid Regional Ministry of Education, Ministry of Economy and Business, Huawei, European Space Agency (ESA), SENER, and other private companies with a total fund exceeds 2.5 million Euros. His technical interests include antennas and propagation, ultrawideband/multiband antennas, reflector/feed systems, radio astronomy receivers, base stations, 5G communications, antenna arrays, THz technologies, whispering gallery mode resonators, and millimeter/submillimeter waves.

Mr. Abdalmalak received the Erasmus Mundus GreenIT Grant, in 2014, and the Young Scientists Award (Second Prize) by URSI/Spain, in 2017. He was selected as an IEEE Ambassador for the IEEEXtreme 14.0 Competition at Region 8 (Europe, Middle East, and Africa), in 2020, and the IEEE Section Lead for Spain for the IEEEXtreme 15.0 Competition, in 2021. He served as a TPC Member/Peer Reviewer for several JCR journals and international conferences, such as IEEE Access, *Optics Express*, *Progress in Electromagnetics Research* (PIER), the *International Journal of Infrared and Millimeter Waves* (IJIM), the European Conference on Antennas and Propagation (EuCAP), ITCE, ICEECC, AsiaSim, and CIAP.

DANIEL SEGOVIA-VARGAS (Member, IEEE) was born in April 1968. He received the Telecommunications Engineering degree from ETSIT, UPM, in 1993, the Ph.D. degree *(cum laude)* in telecommunications engineering from ETSIT-UPM, in 1998, with a distinction by unanimity, and the Doctor Honoris Causa degree from Universidad Católica San Pablo, Arequipa.

From 1993 to 1998, he was an Assistant Professor at the Universidad de Valladolid. Since 1998, he has been a Professor at the Universidad Carlos III de Madrid (UC3M). Since 2001, he has been an Associate Professor (Tenure) of signal theory and communications at the signals at UC3M, where he is currently teaching high-frequency microwave and circuits and antennas. Since 2003, he has been chairing the Radiofrequency, Electromagnetics, Microwaves, and Antennas Group (GREMA), UC3M. From 2004 to 2010, he was the Head of telecommunications engineering at the Escuela Politécnica Superior, UC3M. From 2012 to November 2020, he was the Head of Escuela Politécnica Superior, UC3M. He has been a Full Professor at UC3M, since 2016. He has been a Visiting Researcher at the Rutherford Appleton Laboratory and CTU in Prague. He has authored or coauthored more than 350 publications in scientific journals and international conferences (more than 90 in indexed international journals and more than 20 international invited conferences). His research interests include antennas (antenna arrays and miniaturized antennas, where he has led different projects with outstanding companies, such as Airbus, Repsol, or Indra), active antennas, metamaterials, and technologies in THz frequencies. He has been a member of AP-S Society, since 1998, and MTT-S Society, since 2001. He has been the Treasurer of the European Microwave Conference, in 2018, and Eucap 2022 in Madrid. He received the Best Thesis Award in mobile communication by COIT-Ericsson for his Ph.D. degree. He was the Chairperson of URSI2011 and a member of the Organizing Committee of Eucap 2010 (where he was the Awards Committee). He has organized several international workshops in the domain of metamaterials and THz technologies. He has been chairing courses in the European School of Antennas, since 2013. He has been the National Delegate for European Cost actions in the antennas field (Cost 284, Cost IC0603, and Cost IC1102), since 2002. He has chaired more than 80 research and development projects, both public and private. Since 2013, he has been a Treasurer and a Secretary of the IEEE Spanish Chapter.